



Annealing temperature effect on properties of chemically deposited PbTe films and bulk

Ghassan Nashed*

Department of Physics, Collage of Sciences, University of Aleppo (SYRIA)

E-mail: Ghassan-n@hotmail.com

ABSTRACT

The PbTe films were deposited onto glass substrate (microscopic slices) by a chemical bath method (CBD) at room temperature. The deposited films are dense, smooth, and uniform with silver gray metallic luster structure. Using XRD, it found that the structure of PbTe possesses stable face centered cubic (fcc) phase. The grain size of the PbTe bulk increased within the range of 33– 57 nm with annealing temperature increasing. AFM micrographs of surface of the prepared film are observed that horizontal distance in the rang (230– 395) nm. The band gaps of the PbTe are determined from UV-Vis spectrophotometer and are found to be within the range (0.39 - 0.95) eV. Energy band gab of PbTe which determined from FT -IR spectrophotometer is (0.36ev). The activation energy varied from 0.35- 1.72 eV for films and from 0.11-0.34 eV for bulk with annealing temperature variations from 373-573K. Films and bulk exhibit p-type conduction and resistivity in the range ($75 \times 10^{-4} \Omega \cdot \text{cm}$ - $146 \times 10^{-4} \Omega \cdot \text{cm}$). The carriers density and Hall mobility in PbTe bulk were in the rang $5.8 \times 10^{23} \text{ m}^{-3}$ and $4.004 \text{ m}^2/\text{Vs}$. © 2015 Trade Science Inc. - INDIA

KEYWORDS

Lead telluride;
CBD method;
Hall effect;
Impedance spectroscopy.

INTRODUCTION

Lead chalcogenide Semiconductor have attracted more attention in the past few decades, in both fundamental research and technological applications, because of their controllable size dependent electronic and optical properties. Recently, the synthesis of nanostructured semiconductor materials with controlled morphologies such as films, quantum dot, nano rod, nanowire, etc. It found that finds applications in optoelectronics, biotechnology, catalysis, etc.^[1,2]. Lead chalcogenide materials (PbS, PbTe and PbSe) exhibit properties, which are unusual and possibly unique,

relative to other semiconductors. Particularly, unusual feature of this group of materials is the relative stability of the lattice over a wide range of non-stoichiometry. Compared with values for other semiconductors^[3]. As one of the important IV–VI semiconductor materials, the rock-salt (face centered cubic) structured lead telluride (PbTe), PbTe structure has been the object of particular attention, because of its narrow band gap of 0.32 eV (in the bulk at room temperature). The unusual characteristics of lead salt PbTe such as high carrier mobility, narrow band gap make them unique among polar compound and have important application in many fields, such as light emitting

Full Paper

diodes and infrared laser in fiber optics, thermoelectric devices and infrared detection^[4,5]. PbTe have potential applications in power generation and thermal sensing. Theoretical calculation and experiments indicate that improvement in Te properties can be achieved as the dimensionality of materials is reduced^[6,7]. Low dimensional Te materials such as films are of great interest for construction of high performance Te devices. In addition, PbTe films are also good candidates for optoelectronic applications in the mid-infrared range^[8]. Various methods have been utilized to prepare PbTe thin films, such as vacuum evaporation^[9,10], magnetron sputtering^[11], molecular beam epitaxy^[12], pulsed laser deposition^[13], hot-wall epitaxy^[14,15], and electro deposition^[16]. All these methods need special equipment's, and the electro deposition method needs conductive substrates, although it is relatively low-cost. Chemical bath deposition (CBD) method does not have special requirement for substrate and does not need special equipment. This is the technique possesses a number of advantages such as low cost, low working temperature, and easy coating of large surfaces, over other film deposition methods^[17]. CBD technique is very suitable method for deposition of polycrystalline PbTe films with good photoconductive properties^[17]. The photoconductive effect of PbTe films may be attributed^[18] to an amorphous to crystalline transformation during annealing process. It has been found that the properties of chemically deposited PbTe films depend strongly on the growth conditions such as PH deposition, temperature, deposition time, and annealing temperature^[19]. In this work, PbTe films were deposited on glass substrate, at room temperature, in an alkaline aqueous solution and as a powder, by a CBD method. Optical properties of this film was studied via absorption spectrum. After preparation, PbTe samples were pressed in disk shape. Structural properties of PbTe has been studied by X-ray diffraction (XRD). DC and Hall effects measurements were carried out.

EXPERIMENTAL

Preparation of PbTe

Substrates Cleaning

The cleaning of the substrate surface is significant for the characteristic of the film structure. Microscopic slices glass substrates were cleaned using an oxidant mixture ($K_2Cr_2O_7:H_2SO_4 - 1:10$, HNO_3 , 1% EDTA) then rinsed with distilled water and dried.

Film preparation

The lead telluride films were deposited by the (CBD) method. For deposition of PbTe films, lead acetate was used as Pb^{2+} and telluride oxide as Te^{2+} source in an alkaline medium. solution, prepared by taking 1mmol of lead acetate $Pb(CH_3COO)_2 \cdot 3H_2O$ dissolved in 20 ml of distilled water, stirred for 10 min, 1 mmol of TeO_2 , 0.02 mol of KOH and 2 mmol of trisodium citrate (TSC) dissolved in 100 ml of deionized water then it stirred for 15 min, all constituents were mixed together. While the solution was stirred we added 8 mmol of KBH_4 , within a few seconds color of the solution turned dark brown indicating complete dissolution of KBH_4 , and the solution was continuously stirred for 30 min. pH (11.5) and temperature (407K) were kept constant for all depositions. The solution was diluted to 200 ml in a beaker and then was placed at room temperature without stirring. Two Microscope glass slide was used as the substrate after being cleaned by the method mentioned above. The slide was put in the solution at an angle of 30 to the bottom of the beaker. The solution gradually turned dark. About 72 h later. The reaction process of deposition of PbTe as following:

- 1) $Pb^{2+} + 3OH^- \rightarrow HPbO_2^- + H_2$
- 2) $TeO_2 + 2OH^- \rightarrow TeO_3^{2-} + H_2O$
- 3) $HPbO_2^- + H_2O \rightarrow Pb^{2+} + 3OH^-$
- 4) $Pb^{2+} + TeO_3^{2-} \rightarrow PbTeO_3$
- 5) $2PbTeO_3 + 6BH_4^- \rightarrow 2PbTe + 6OH^- + 3B_2H_6 \uparrow$

The $Pb(Ac)_2$ and TeO_2 were dissolved in excess alkali and form $HPbO_2^-$ and TeO_3^{2-} ions, according to reactions (1) and(2), respectively. The TeO_3^{2-} , $HPbO_2^-$ and BH_4^- (from KBH_4) all are negative charges; therefore, the reduction reactions related to them are difficult. Some $HPbO_2^-$ ions are hydrolyzed into Pb^{2+} (reaction (3)). The Pb^{2+} combines with the TeO_3^{2-} to form $PbTeO_3$ colloidal particles (reaction (4)). The $PbTeO_3$ colloidal particles

are reduced into PbTe by BH_4^- (reaction(5)) and PbTe nuclei form. The PbTe nuclei attach to the surface of the substrate, and on the wall of the beaker grow up and form films, and the PbTe nuclei in the solution grow up slowly as powder and precipitate at the bottom of the beaker. The deposition procedure was carried out at room temperature; therefore, the growth of the PbTe nuclei should be very slow.

The silver gray film deposited on the downward side of the substrate was more strongly adhered while that on the upward side was weakly adhered. Therefore, hereinafter, only the film deposited on the downward side of the substrate was further studied. It was heated at 473K temperature for 30 minutes and kept at room temperature for further measurements. Black powder precipitated on the bottom of the beaker was collected. The powder was washed with distilled water and ethanol several times, then dried at 343K for 4h, The formed powder was milled by a ceramic mortar, pressed under 7 ton/cm² as 3 disks of 22.3 mm diameter and 1.5mm thickness. Then disk samples were annealed at 373, 473, 573K temperature for 30 minutes. Structural characteristics of the bulk materials were determined by X-ray diffraction (XRD) method using Philips X-pert Pro diffract meter at room temperature with Cu-K α radiation ($\lambda=1.54 \text{ \AA}$). Optical absorption spectra of the films were taken via a UV spectrophotometer in the wavelength range (300 to 900) nm. Disks were polished and washed by alcohol. In

addition, an air-dry silver pastes were applied to the samples surfaces as electrodes, to ensure a good electrical contact and introduce them for further characterization

RESULTS AND DISCUSSION

XRF spectrum

Using XRF device, Unisantis® type Si-PIN with molybdenum (Mo) target operated at 50kV and 1mA, XRF spectrum was taken for the prepared sample before heat treatment.

Figure 1 shows the peaks related to existence of Pb and Te with percentage of 67.74% of Pb and 30.4% of Te with toxic elements as it shown in TABLE 1. The XRF measurements confirm the reaction ratio of Pb : Te

Structural study

Figure 2 Shows the XRD spectrum of three samples of PbTe in discs form, annealed at 373, 437, and 573 K for 1h. Figure 2 shows several diffraction peaks at 2θ values of 24.1, 27.5, 39.6, 49.5 and 64.3. Which correspond to (111), (200), (220), (222) and (420) planes of the face-centered-cubic (fcc) rock-salt structure of PbTe. Where some of orientation plane are missing in spectrum of sample treated at 373K (Figure 2a)

Scherrer's formula was used to calculate crystallite size^[20, 21]:

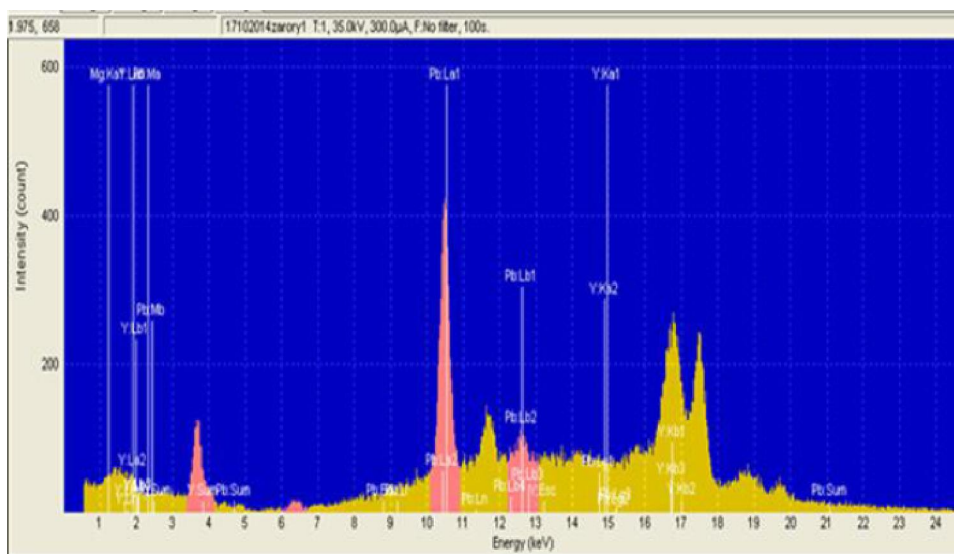
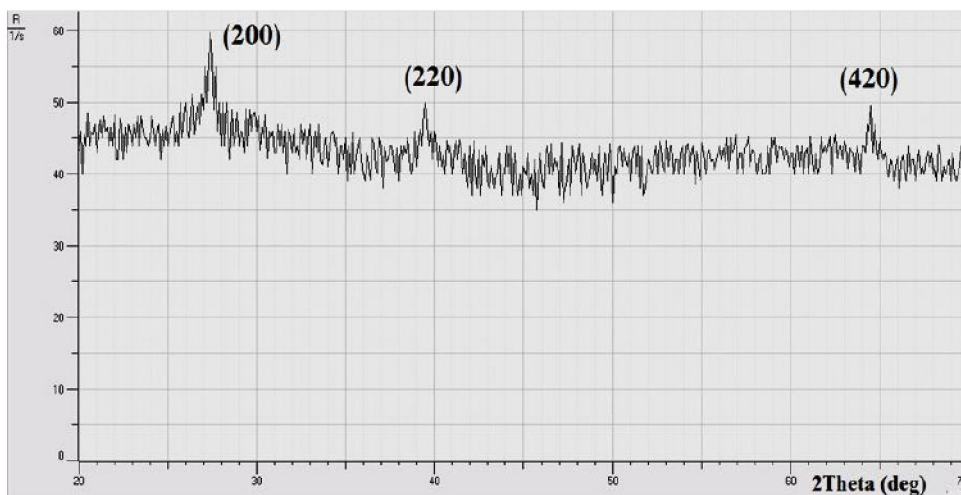


Figure 1 : XRF spectrum for PbTe sample

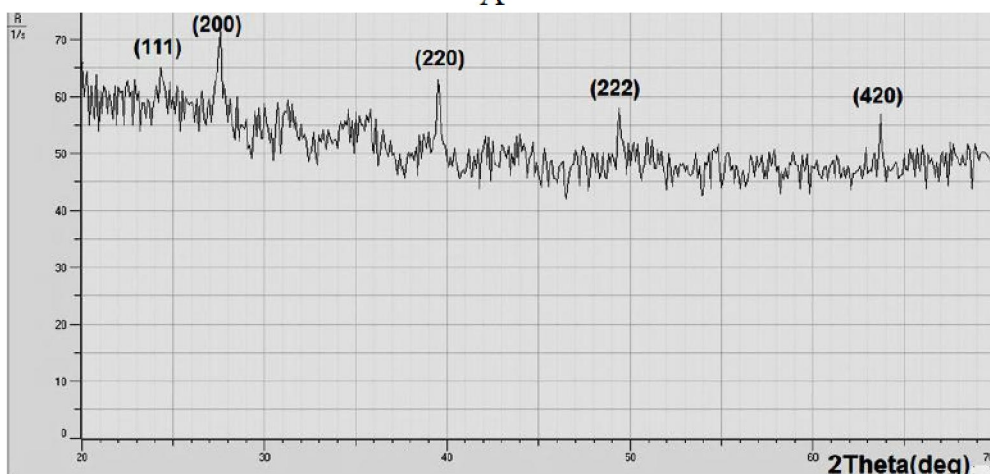
Full Paper

TABLE 1 : Percentage of elements as result of XRF spectrum for PbTe sample

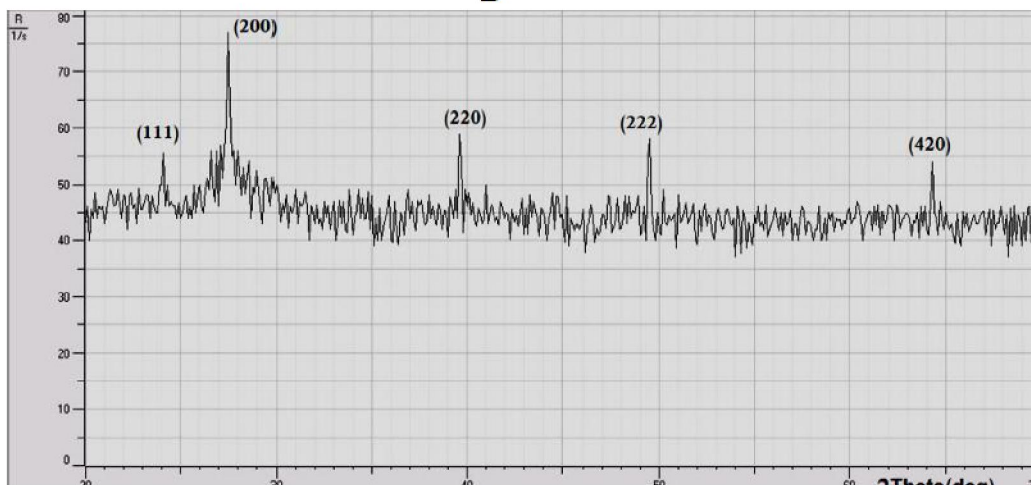
Element	Pb%	Te%	Fe%	Kr%
Concentration	67.739	30.371	1.412	0.479



A



B



C

Figure 2 : The XRD profile of PbTe sample at various temperatures a) at 373K B) at 473K C) at 573K

$$D = K \lambda / (\beta_{20} \cos \theta) \quad (1)$$

Where K is a constant taken to be 0.94, λ is the wavelength of X-ray of Cu-K α radiation ($\lambda = 1.54\text{\AA}$) and β_{20} is the full width at half maximum (FWHM) of the diffraction peak corresponding to a particular crystal plane. The strain (ϵ) was calculated by the following expression^[22]:

$$\epsilon = \beta_{20} \cos \theta / 4 \quad (2)$$

The dislocation density (δ), defined as the length of dislocation lines per unit volume of the crystal, was evaluated from the formula^[22]:

$$\delta = 1/D^2 \quad (3)$$

TABLE 2 summarizes the calculated values of crystallite size (D nm), strain (ϵ), dislocation (δ), and lattice constant (a).

It can be noticed from TABLE (2) that the crystallite size increases with increasing annealing temperature. In contrast, the strain and dislocation decrease with increasing annealing temperature. This means that the thermal treatment increases the relaxation.

Thin film morphology

TABLE 2 : XRD profile results at various temperatures

Sample	0C	D nm	$\epsilon \times 10^{-4}$ lines-2. m-4	$\delta \times 10^{13}$ lines/m ²	a (Å)
1	100	33	50.55	91.82	3.02
2	200	49	33.99	41.64	3.02
3	300	57	29.14	22.95	3.02

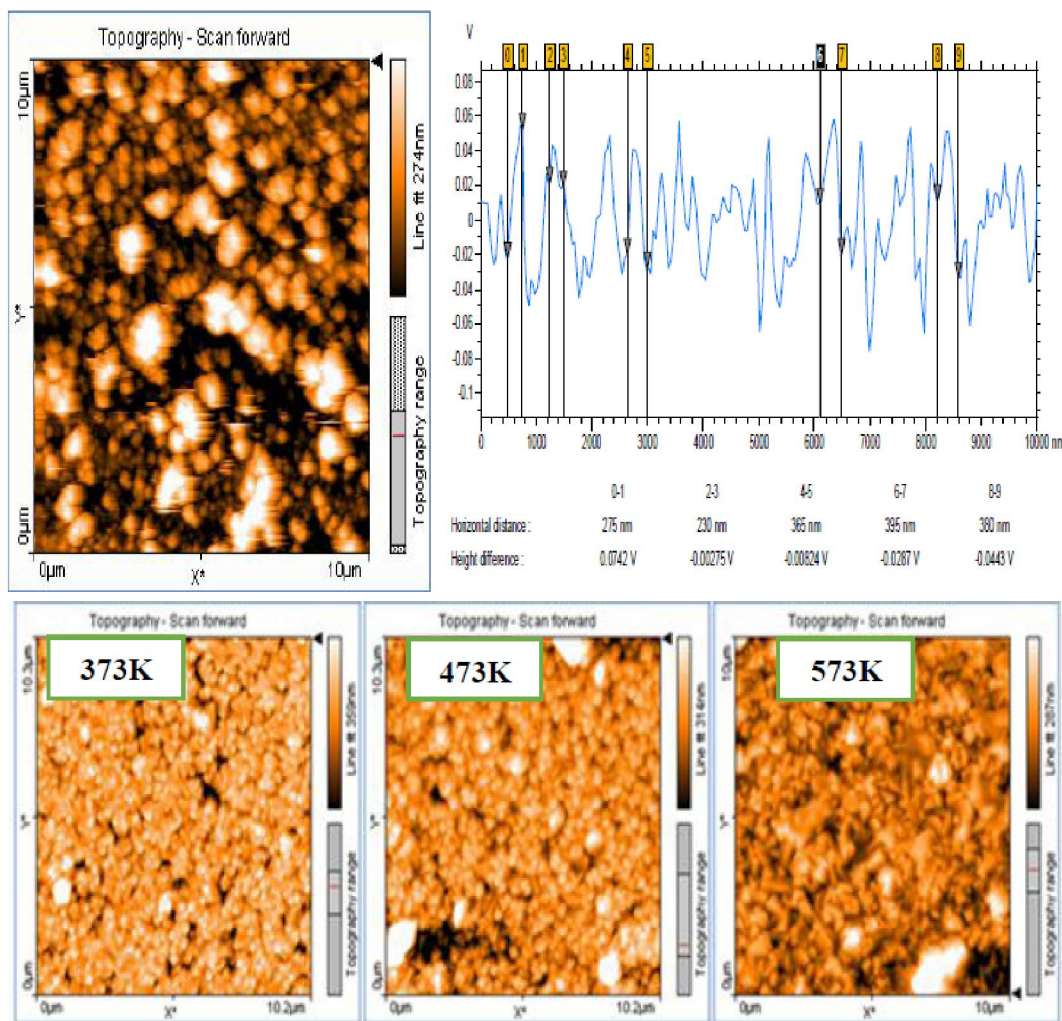


Figure 3 : AFM micrographs of PbTe treated at different temperature

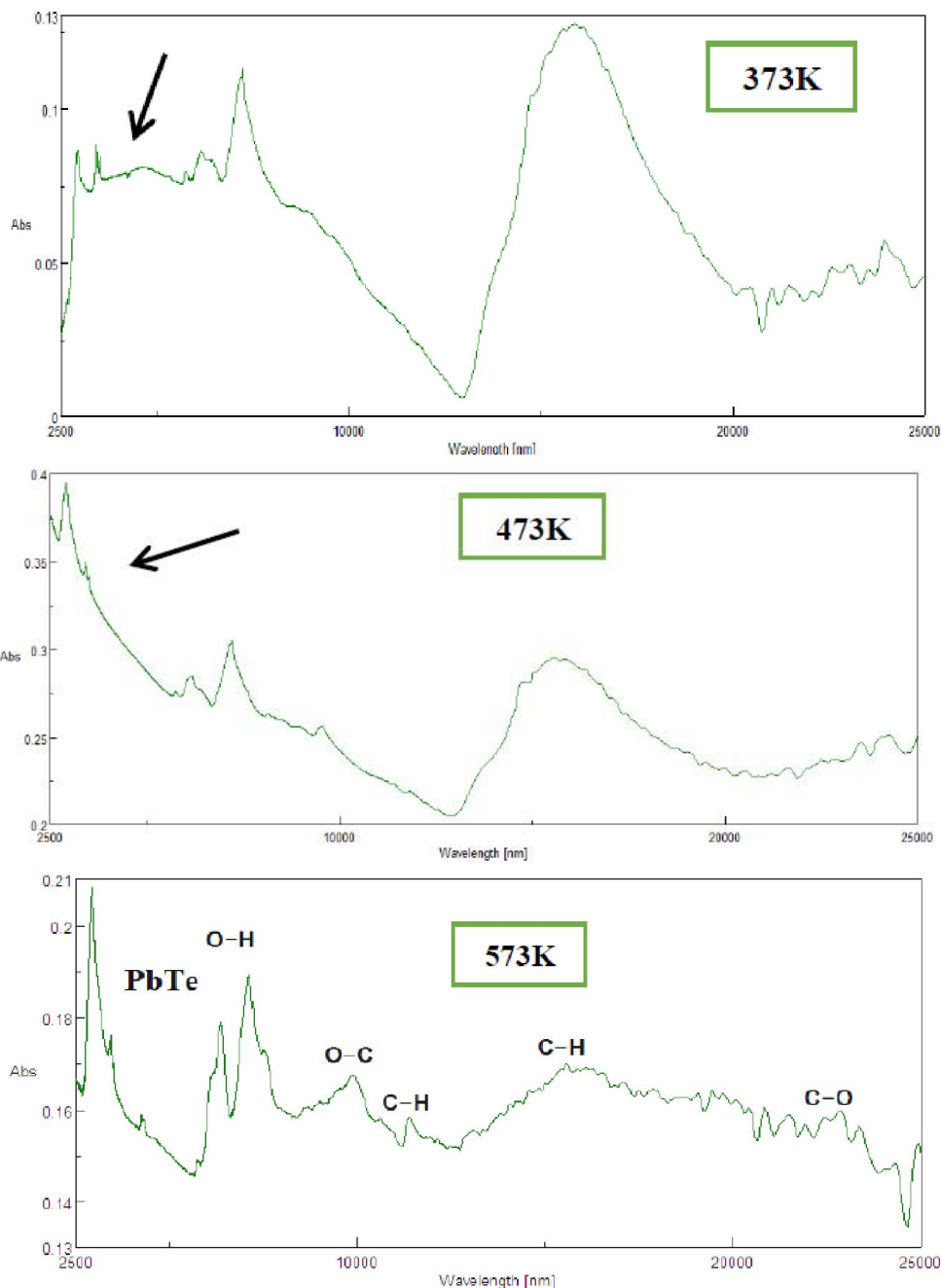


Figure 4 : IR absorption of PbTe treated at three different temperatures in the wavelength range (2500-25000) nm

Figure 3. Shows the morphology of films deposited at 30°C and annealed at 373, 473, and 573K taken by AFM. We note that the surface of the film have a form of granules with different sizes vary between (230 – 395) nm. Also one can observe that the grain size increases with heat treatment temperature.

It can be observed that the surface of the films is not very compact. Small crystallites or grains compose them. Round shaped clusters packed together

constitute the films. This cluster appearance caused by size of the clusters increases with annealing temperature and many empty spaces can be seen between these clusters. The average grain size is about 287 nm.

Optical Properties

FT- IR measurement

Figure (4) show the FT- IR absorption in function of wavelength range (2500 -25000 nm) for the

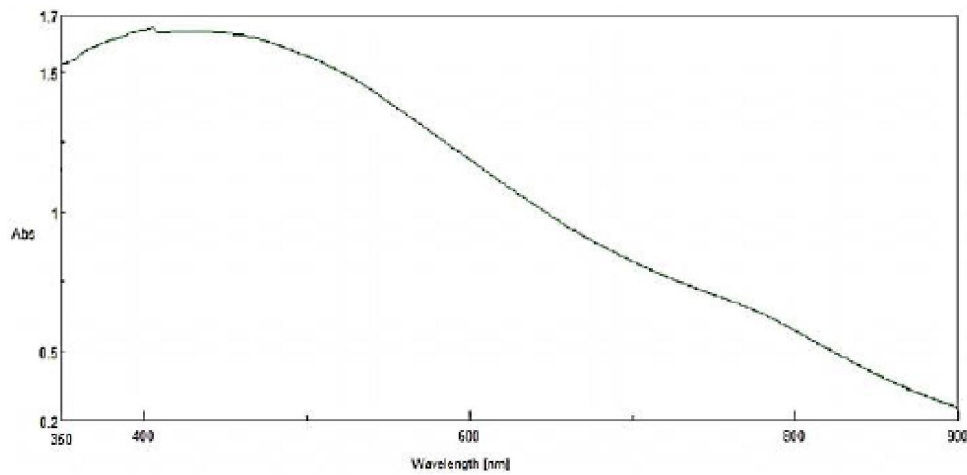
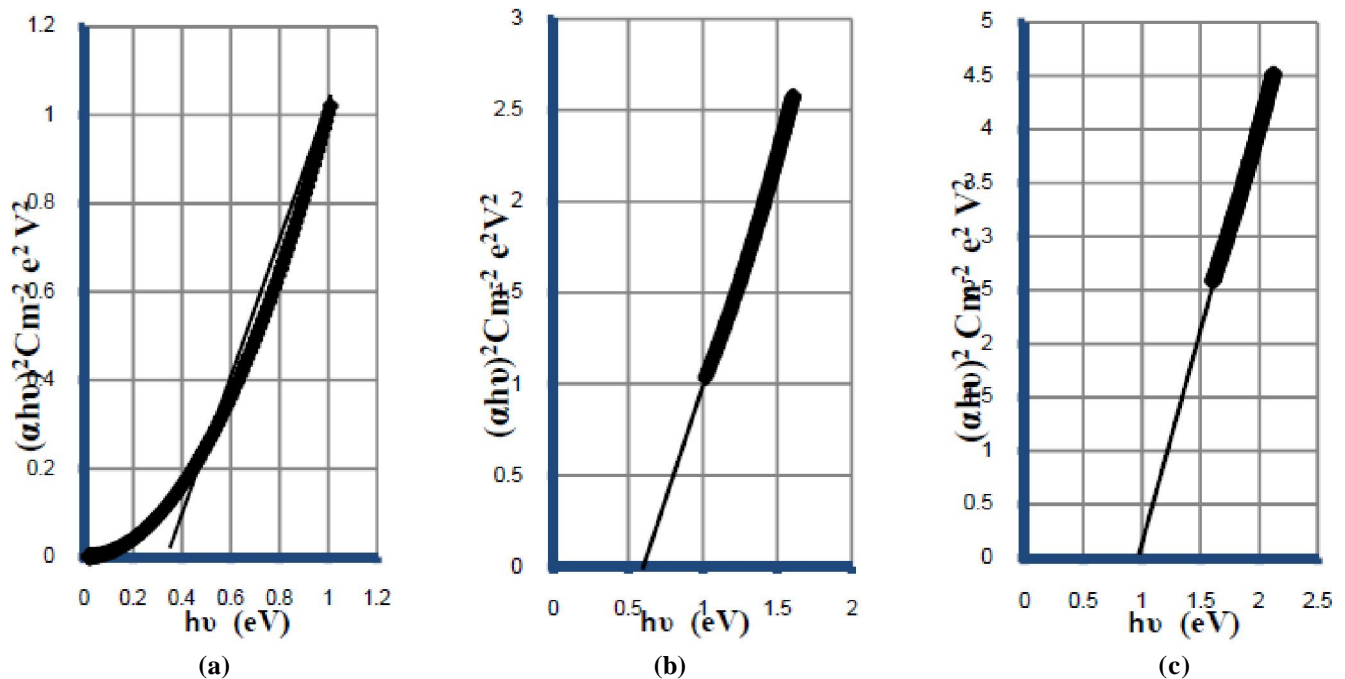
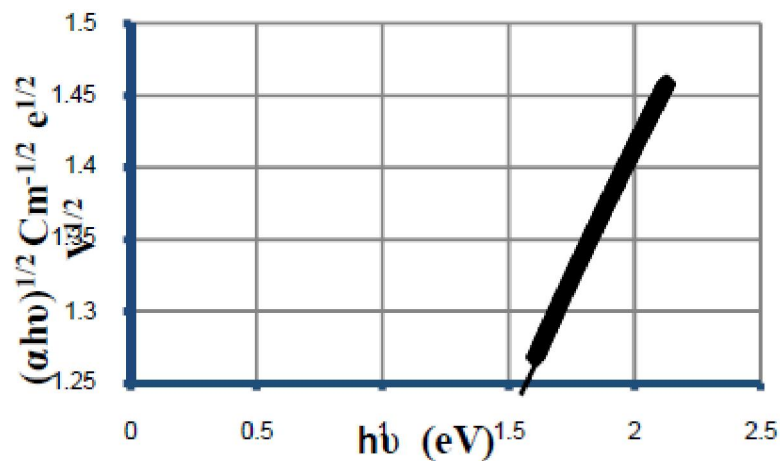


Figure 5 : Absorption spectra of PbTe thin film

Figure 6 : $(\alpha h\nu)^2$ in function of $h\nu$ where:(a) (416 to 550) nm, (b)(551 to 689) nm, and(c)(690 to 900) nmFigure 7 : $(\alpha h\nu)^{1/2}$ in function of $h\nu$ in range(690 to 900) nm

Full Paper

three samples treated at three different temperatures. They indicate that the energy band gap is (0.36eV) which corresponds to wavelength (3418.24nm). The other peaks are due to the residual O-H, C=O, C-H, and O-C. It can be noticed from Figure 4. that the toxicity diminishes with increasing heat treatment temperature.

UV-Visible spectrum

The optical absorption of PbTe thin films was studied in the wavelength range 350 to 900 nm. As it shown in Figure 5, PbTe film shows higher absorption at shorter wavelength side.

Energy band gap can be calculated using Tauc formula^[23]:

$$(\alpha h\nu)^{1/n} = A [h\nu - E_g] \quad (4)$$

Where A is constant, E_g is the band gap of the film. The exponent n depends on transition type. The values of n for direct allowed, indirect allowed, and direct forbidden transmissions are $n = 1/2, 2,$ and $3/2,$ respectively. The direct band gaps were obtained from the linear portion of $(\alpha h\nu)^2$ vs. $h\nu$ plot as shown in Figure 6, which lie in the range 0.39 – 0.99 eV. The indirect band gaps were obtained from the $(\alpha h\nu)^{1/2}$ vs. $h\nu$ plot as shown in Figure 7. Its value is 1.55eV. While there is no direct forbidden transition. It found that direct band gap is higher than that

of bulk value of PbTe (0.34 eV) because of the grain size effect of PbTe.

Electrical Measurements

AC measurements

AC measurement carried out using GAIN PHASE ANALYZER (Schlumberger - SI1253). Thin film complex impedance spectrum was taken for thin film in frequency range (1Hz – 20KHz) at constant voltage ($v = 5V$) and at different temperature (373, 473 and 473K). Figure (8) shows the relationship between the imaginary part $X(\omega)$ and the real part $R(\omega)$ of the complex impedance.

$$Z(\omega) = R(\omega) + j X(\omega) \quad (5)$$

We note that impedance spectrum has a semi-cycle due to Debye model which indicates that the grains are deviated from homogeneity and the equivalent circuit consists of capacitance in parallel with resistance. It's noticeable when $R(\omega)=0, X(\omega)\neq 0,$ that mean at frequency equals to 0 Hz, free charges presented at the surface of the sample.

DC measurements

(I – V) characteristics

(I – V) characteristics of three samples thin film of PbTe annealed at 373 - 473 -573 K for 1h were carried out. Figure 9. Shows that the relationship

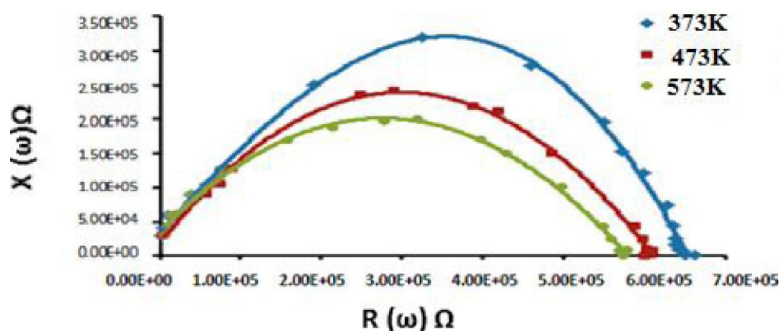


Figure 8 : The relationship between the imaginary part $X(\omega)$ and the real part $R(\omega)$ of the complex impedance

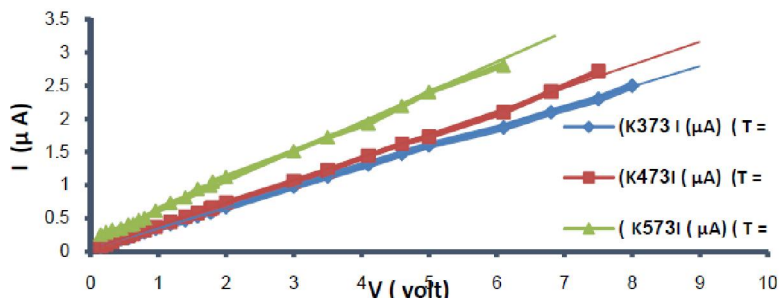


Figure 9 : The (I – V) characteristics of PbTe thin film at different temperatures

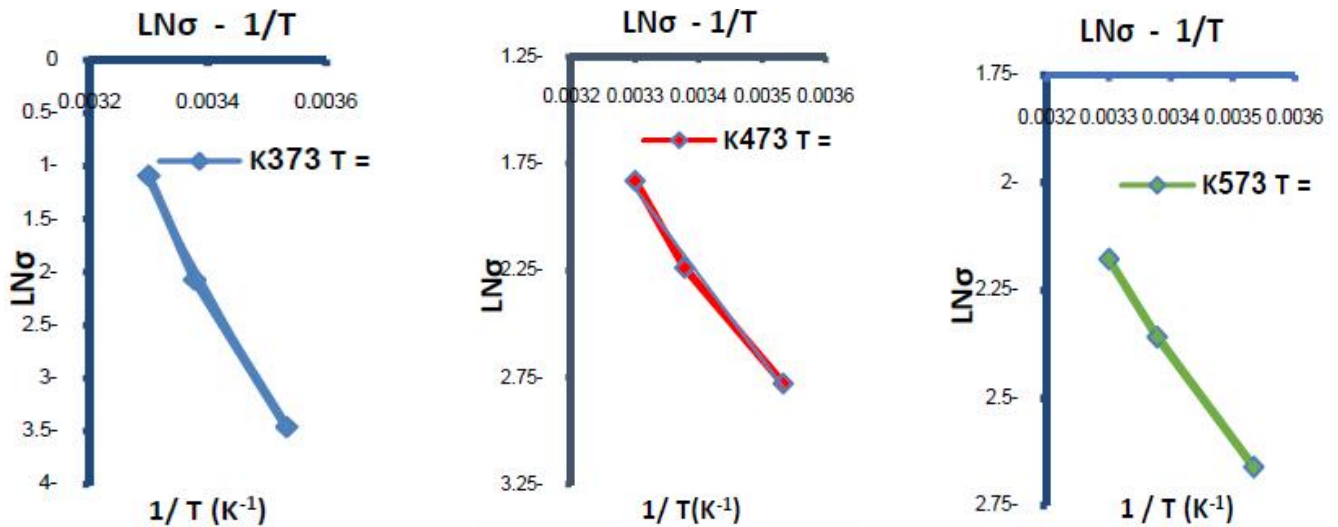


Figure 10 : $\ln(\sigma)$ as a function of $1/T$ (K^{-1}): (a). annealing at 373 K, (b). annealing at 473K, (c). annealing at 573 K

TABLE 3 : Activation energy with annealing temperature for PbTe film

Sample	Annealing temperature(k)	Ea. (ev)
1	373	1.72
2	473	0.68
3	573	0.35

TABLE 4 : Activation energy with annealing temperature for PbTe bulk

Ea. (eV)	Annealing temperature (K)	Sample
0.34	373	1
0.25	473	2
0.11	573	3

between I and V is approximately linear.

Activation energy

For PbTe thin film

The variation of electrical conductivity of semiconductor in function of $1/T$ is given by:

$$\sigma = \sigma_0 \exp(E_a/kT) \quad (6)$$

Where, σ is conductivity at temperature T , σ_0 is a constant, k is Boltzmann constant and E_a is the activation energy. Figure 10. Shows $\ln \sigma$ in function of $1/T$ for the three thin film samples annealed at three different temperatures.

TABLE 2. Shows that the calculated activation energy for the three samples decrease from (0.35 to

1.72) eV as annealing temperatures increase. This means that the change in activation energies may refer to the structural improvement due to eliminate defect through annealing.

The change of activation energy E_a attributed to the variation of barrier height when the film samples annealed at different temperature.

For bulk PbTe

Figure 10 shows the (I-V) characteristics of PbTe bulk at different annealing temperatures.

TABLE 4. Gives the variation of activation Energy with annealing temperature for PbTe bulk samples calculated as it was mentioned above.

It can be noticed that activation energy decrease

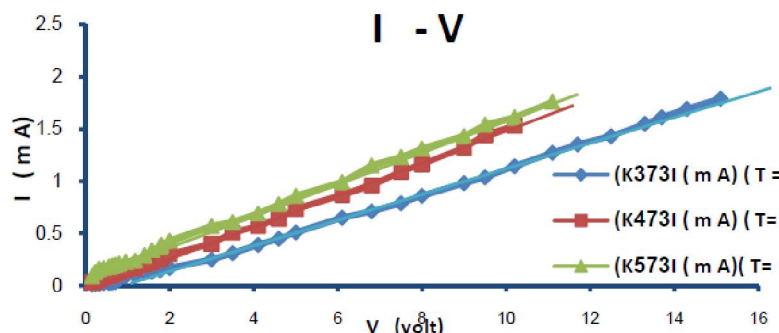


Figure 11 : The (I -V) characteristics of PbTe bulk at different temperature

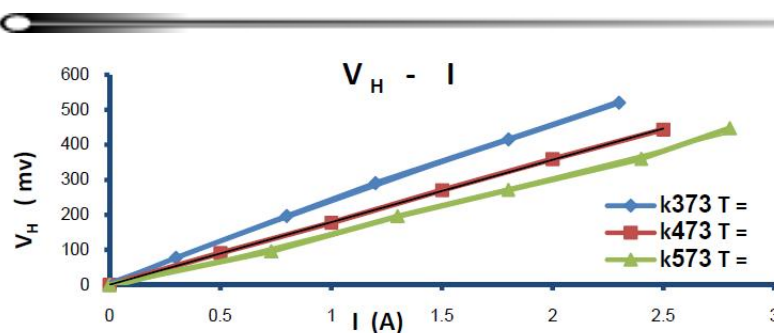
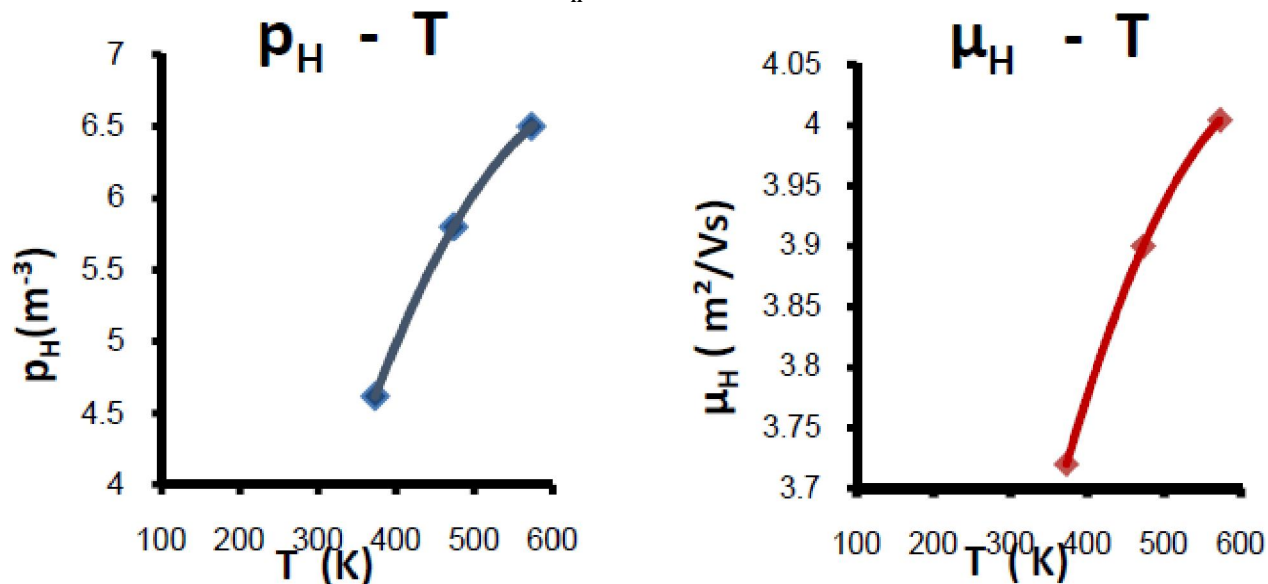
Figure 12 : Hall voltage (V_H) with the current for PbTe thin filmsFigure 13 : Carrier concentration (P_H) and Hall mobility (μ_H) with annealing temperature for PbTe bulk

TABLE 4 : Values of parameters resulting from Hall Effect studies

Sample	1	2	3
Degree annealing (K)	373	473	573
Hall coefficient $R_H \times 10^{-6}$ (m^3/C)	1351	1069	949
Carrier density $P_H \times 10^{23}$ (m^{-3})	4.62	5.8	6.5
Resistivity $\rho \times 10^{-6}$ (Ω)	337.8	287.2	237
Hall mobility μ ($m^2/V s$)	3.729	3.998	4.004

with annealing temperature increasing. This reduction can take the same interpretation of the thin film.

Hall effect measurements

The variation of Hall voltage (V_H) with current for PbTe bulk samples annealed at 373, 473, 573 K is shown in Figure 12. Hall effect reveals that the prepared thin PbTe films are p-type due to sulfide ions vacancies^[24] that means the conduction is dominated by holes^[25].

The variation of carrier concentration (P_H) and Hall mobility (μ_H) with annealing temperature for PbTe bulk are shown in Figure 13. It was found that the carriers concentration decrease with increasing

annealing temperature while Hall mobility increases with the annealing temperature increasing are shown in TABLE 4.

CONCLUSIONS

CBD chemical method was an effective, easy and cheap way to deposit PbTe Thin films. XRF showed that the prepared samples were closed to stoichiometry. XRD showed that the higher the annealing temperature, the less strain and dislocations. FT-IR revealed the existence of some toxicity in the prepared samples. Activation energy showed decrease with increasing annealing temperature both

for thin films and bulk sample. AFM micrograph and Impedance spectrum showed that there is no homogeneity in the bulk and thin film samples. Hall measurements confirmed *p*-type conduction for PbTe films deposited on the glass substrate. The carrier concentration was estimated to be about $5.8 \times 10^{23} \text{m}^{-3}$ and the mobility is about $4 \text{ m}^2/\text{V s}$.

ACKNOWLEDGEMENT

I would like to thank Mr. Sami Orfali and M.A. Batal for their technical support, encouragement and unlimited scientific discussions.

REFERENCES

- [1] X. Yang, Z. Yan, L. Jiang, X. Wang, K. Zheng; Synthesis and photo catalysis of Al doped CdS templated by non-surfactant hypocrellins, *Mater Lett.*, **57**, 2755-2760 (2003).
- [2] Q. Zhang, F. Huang, Y. Li; Cadmium sulfide Nano rods formed in microemulsions, *Coll. Surf.*, **497**, 257–258 (2005).
- [3] S. Kumar, Z.H. Khan, M.A. Majeed Khan, M. Husain; Studies on thin films of Leads Chalcogenide, *Current Applied Physics*, **5**, 561 (2005).
- [4] I.N. Chao, P.J. McCann, W.L. Yuan, E.A. O'Rear, S. Yuan; Structural, Electrical, and Optical Properties of PbTe Thin Films Prepared by Simple Flash Evaporation Method, *Thin Solid Films*, **323**, 126 (1998).
- [5] I. Pop, C. Nascu, V. Ionescu, E. Indrea, I. Bratu; Structural and optical properties of PbS thin films obtained by chemical deposition, *Thin Solid Films*, **307**, 240 (1997).
- [6] T.C. Harman, P.J. Taylor, M.P. Walsh, B.E. LaForge; Quantum dot superlattice thermoelectric materials and devices, *Science*, **297**, 2229 (2002).
- [7] L.D. Hicks, T.C. Harman, X. Sun, M.S. Dresselhaus; Low dimensional thermoelectric materials, *Phys.*, **104**, 93 (1996).
- [8] S.S. Sahay, S. Guruswamy, J. Mater; Expitaxial growth of PbTe film on Si substiate, *Sci. Lett.*, **17**, 1145 (1998).
- [9] T. Komissarova, D. Khokhlov, L. Ryabova, Z. Dashevsky, V. Kasiyan; Impedance of photosensitive nanocrystalline PbTe(In) films, *Phys. Rev. B*, **75**, 1-5 (2007).
- [10] M. Ito, W.S. Seo, K. Koumoto, J. Mater; Thermoelectric properties of PbTe thin films prepared by gas evaporation method, *J. Mater. Res.*, **14**, 209 (1999).
- [11] A. Jdanov, J. Pelleg, Z. Dashevsky, R. Shneck; Growth and characterization of PbTe films by magnetron sputtering, *Mater. Sci. Eng. B.*, **106**, 89 (2004).
- [12] H. Zogg, K. Alchalabi, D. Zimin; Electrodeposition of PbTe thin films from acidic nitrate baths, *Defence Sci. J.*, **51**, 53 (2001).
- [13] A. Jacquot, B. Lenoir, M.O. Boffou, A. Dauscher; Facile synthesis of thermoelectric films via spin-coating metastable precursors, *Appl. Phys. A Mater. Sci. Process.*, **69**, 613 (1999).
- [14] M.K. Sharov, Y.A. Ugai, J. Surf; Facile synthesis of PbTe nanoparticles and thin films in alkaline aqueous solution at room temperature, *Invest.*, **2**, 481 (2008).
- [15] H. Y. Chen, S.S. Dong, Y.K. Yang, D.M. Li, J.H. Zhang, X.J. Wang, S.H. Kan, G.T. Zou; The effect of high pressure on the emissions of Eu^{3+} in cubic Y_2O_3 and Gd_2O_3 hosts *J. Cryst. Growth*, **273**, 156 (2004).
- [16] H. Saloniemi, T. Kanninen, M. Ritala, M. Leskela; Electrodeposition of PbTe thin films, *Thin Solid Films*, **326**, 78 (1998).
- [17] F.I. Ezema, R.U. Osuji; Perpatation and optical characterization of chemical bath deposited, *Journal Applied Sciences*, **6**, 1827 (2006).
- [18] E. Pentia, L. Pintilie, T. Matei, E. Botila, E. Ozbay; Chemically prepared nanocrystalline PbS thin film, *Journal of Optoelectronics and Advanced Materials*, **3**, 525 (2001).
- [19] R.S. Parra, P.J. George, G.G. Sanchez, G. Jimenez, L. Banos, P.K. Nair; Analysis of thin chalcogenide PbS films prepared from chemical bath, *Journal of Physics and Chemistry of Solids*, **61**, 659 (2000).
- [20] V.M. Garcia, M.T.S. Nair; P.K. Nair; Optical properties of PbS-CuxS and Bi2S3-CuxS thin films, *Sol. Energy Mater.*, **23**, 47–59 (1991).
- [21] V. Stancu, M. Buda, L. Pintilie, I. Pintilie, T. Botila, G. Iordache; Chemically prepared nanocrystalline PbS thin films, *Thin solid films*, **516**, 4301-4306 (2008).
- [22] A.U. Ubale, A.R. Junghare, N.A. Wadibahsmi, A.S. Daryapurkar, R.B. Manker, V.S. Sangawar; Some electrical properties of thin PbS films, *Turk Journal of Physics*, **31**, 279-286 (2007).
- [23] J.I. Pankove; Optical processes in semiconductors, *Prentice-Hall Inc, Englewood Cliffs, NJ* (1971).
- [24] B. Neha, V. Rajiv, S.G. Patel, A.R. Jani; X-Ray diffraction studies of NbTe₂ single crystal, *Bulletin of Material Science*, **27**, 23 (2004).
- [25] M.Z. Obida, H.H. Afify, M.O. Abou-Helal, H.A.H. Zaid; Nanocrystalline anatase titania thin films synthesized by spray pyrolysis for gas detection, *Egypt Journal of Solids*, **28**, 1 (2005).